Very high energy photons and neutrinos: Implications for UHECR

Thomas K. Gaisser[1,a]

Bartol Research Institute and Dept. of Physics and Astronomy
University of Delaware, Newark, DE 19716 USA

Abstract. Depending on the environment of the acceleration processes for ultra-high energy cosmic rays, photons and neutrinos may be produced by interactions in the sources. If so, observations of gamma-rays or neutrinos could pinpoint the sources. This paper reviews some aspects of the search for photons and neutrinos from possible sources of ultra-high energy cosmic rays.

1 Introduction

Both photons and neutrinos are potential tracers of sites of cosmic-ray acceleration because, being neutral, they are not deviated by intervening magnetic fields. Photons are plentiful, but their interpretation is complicated by interactions in the sources and spectral modifications due to cascading in transit. In addition, their origin can be from radiation by electrons as well as from decay of neutral pions. In contrast, high-energy neutrinos would directly imply acceleration of hadrons. Because they interact only weakly, neutrinos are not distorted by interactions in the sources, but for the same reason they are hard to detect. Photons and neutrinos provide complementary types of information about cosmic-ray sources, but they both indicate underlying acceleration of charged particles. It is therefore natural to select known sources of TeV gamma-rays as potential sources of neutrinos.

It is useful to distinguish two ways of producing gamma-rays and neutrinos: at the sources of ultra-high energy cosmic rays (UHECR) and during propagation through the cosmos. In the first case, the observed spectra of the neutral messengers (γ and ν) depend on the source spectrum, on cosmic evolution of the sources and on conditions inside or near the acceleration region. Cosmogenic neutrinos and photons produced during propagation of UHECR depend on the injected spectrum as a function of energy and red shift, but not on conditions at the sources.

It is generally assumed that the highest energy cosmic rays are accelerated in extra-galactic sources, and that the transition from the lower energy population of galactic cosmic rays occurs somewhere between 0.3 and 3 EeV. Protons and nuclei with energies above 30 EeV begin to suffer significant energy losses during propagation from sources more distant than a few hundred Mpc. Ten EeV, being below the suppression energy, but above the transition region is a suitable energy around which to estimate the energy content of the cosmic rays from extra-galactic sources. The observed energy flux at 10 EeV by HiRes [1] and Telescope Array [2] is

$$E\frac{\mathrm{d}N}{\mathrm{d}\ln E} \approx 2\times 10^{-8}\,\mathrm{GeV\,cm^{-2}sr^{-1}s^{-1}}. \tag{1}$$

The range of different measurements is ±50% (higher in AGASA [3] and lower for Auger [4]). Multiplying the energy flux by $4\pi/c$ gives the local energy density in UHECR as 1.3×10^{-20} erg/cm^3 at

[a] e-mail: gaisser@bartol.udel.edu

10 EeV. Dividing by the Hubble time gives an estimate of the power required to supply the UHECR as

$$\frac{\mathrm{d}L}{\mathrm{d}\ln E} \approx 10^{36}\ \mathrm{erg\,Mpc^{-3}}\,s^{-1}. \tag{2}$$

Since the acceleration must extend over several decades of energy, the total power required from the extragalactic sources is $\sim 10^{37}$ erg $\mathrm{Mpc}^{-3}s^{-1}$. Observed densities of various potential sources can be used to estimate the power required for each type of source, as summarized in Table 1.

	Source density (Mpc^{-3}) or rate	av. power required per src. (erg/s)
Galaxies	3×10^{-3}	5×10^{39}
Galaxy clusters	3×10^{-6}	5×10^{42}
AGN	1×10^{-7}	10^{44}
GRB	1000/yr	3×10^{52} ergs/burst

Table 1. Power requirements for some potential sources of ultra-high energy cosmic rays.

Potential sources of UHECR also need to have a combination magnetic field strength B and size R sufficient to allow acceleration to $> 10^{20}$ eV. The condition is [5]

$$E_{\mathrm{max}} \approx \beta(ZeB)R, \tag{3}$$

where β is shock velocity in the case of shock acceleration. Of the potential sources listed in Table 1, galaxy clusters, active galaxies and gamma-ray bursts (GRB) may satisfy this condition (but not by much). As noted already in the original Hillas Plot [5] active galaxies may satisfy the condition in two ways: by acceleration in the compact active galactic nuclei (AGN) or in the radio lobes of giant radio galaxies (i.e. inside the jets close to the central black hole or far out at the termination shock of the jets). This is important in the context of searching for neutrinos from the sources of UHECR because the conditions for neutrino production would be quite different in the two cases. If protons (or nuclei) are accelerated inside the jets of AGN or GRBs, production of neutrinos would be expected by photoproduction on the intense radiation fields there. On the other hand, if the main acceleration occurs at the termination shocks, the amount of neutrino production would depend more on the details of the acceleration process and the environment. In general, one would expect a lower ratio of neutrinos to UHECR in the latter case.

2 TeV observations of active galaxies

Production of TeV photons requires acceleration of charged particles to multi-TeV energies. The observed gamma-rays are usually modeled as originating from electrons, which radiate more efficiently than protons. Protons are likely to be more efficiently accelerated. The extent to which they contribute to the observed photons, and the related question of neutrino production is model-dependent and may vary from one source to another. Despite the uncertainties, it is nevertheless an interesting exercise to compare TeV gamma-ray fluxes from active galaxies with limits from IceCube on neutrino fluxes from the same objects. Fig. 1 makes the comparison for a subset of sources for which there are also IceCube limits [6].

The normalizations and conversion to source luminosity in Fig. 1 are obtained as follows. The TeV gamma-ray flux for Mrk 501 is taken from the quiescent state measurement of VERITAS as cited in Ref. [7], and the normalization for 1ES1959+650 from Ref. [8]. For all others the normalization of the TeV gamma-rays is obtained from the intensity in Crab units quoted in TeVCat [9]. The observed flux in the TeV range is then converted to source γ-ray luminosity with the artificial assumption of a flat νF_ν spectrum from 1 GeV to 1 TeV. IceCube upper limits [10] are converted to source neutrino luminosity assuming an E^{-2} differential neutrino spectrum (flat νF_ν) extending over three decades of energy from

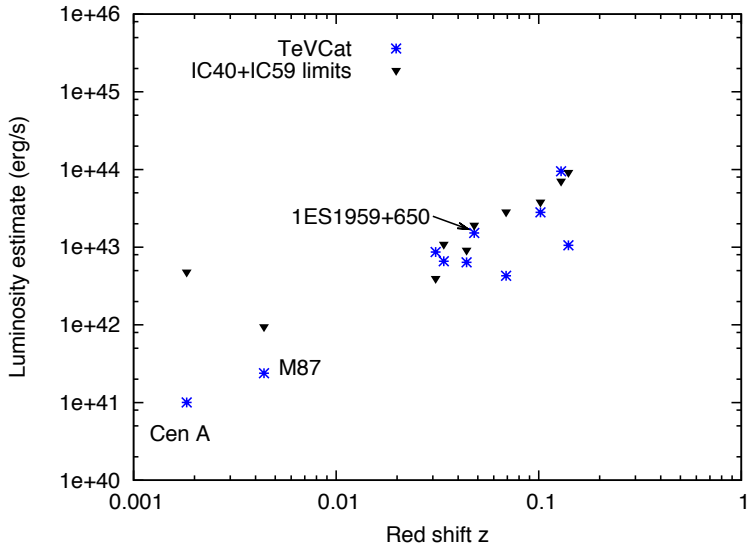

Fig. 1. TeV γ-ray fluxes (asterisks) and IceCube upper limits (inverted triangles) on ν_μ from selected active galaxies. The sources in order of increasing red-shift are Cen A, M87, Mrk-421, Mrk-501, 1ES2344+514, 1ES1959+650, BL Lacertae, W-Comae, H1426+428 and 1ES0229+200. See text for explanation of normalization.

1 TeV to 1 EeV, which corresponds approximately to the region over which IceCube is most sensitive to muon neutrinos from below (Northern hemisphere). All the sources except Cen A and M87 are blazars. A modest beaming factor of $1/4\pi$ is assumed in assigning blazar source luminosities for both photons and neutrinos. The only Southern hemisphere source included is Cen A. The sensitivity region for neutrinos from the Southern hemisphere is much higher in energy as a result of cuts in energy to avoid the large background of atmospheric muons from above. After cuts, the sensitivity region for point sources of neutrinos from the Southern sky is approximately 100 TeV to 100 PeV, and the limit for Cen A is therefore high even though the source is relatively nearby.

The blazar 1ES1959+650 is particularly interesting in the context of a comparison between TeV photons and neutrinos because it has exhibited an "orphan" flare, in which the intensity of TeV photons increased, but not the lower energy photons from the electron synchrotron radiation [11]. Such a flare may be suggestive of a hadronic origin for the TeV gamma-rays[12], in which case neutrinos would also be expected. In 2002 a large flare occurred for both the synchrotron X-ray peak and the high energy, presumably inverse Compton, peak. Two months later the orphan flare occurred only in the high-energy peak [11]. The average TeV photon flux for this source [8], as plotted in Fig. 1 is a factor of three lower than the intensity during the flaring period.

3 Gamma-ray bursts

Passive detectors with large acceptance are better suited to searching for TeV radiation associated with gamma-ray bursts than gamma-ray telescopes, which must be quickly re-oriented to point at the burst. Generally, the limits from telescopes like VERITAS provide limits on photons produced in the afterglow phase of GRBs [13]. Detectors like Milagro [14] and the future HAWC [15] and the neutrino "telescopes", which continuously see a large fraction of the sky, can search retroactively through accumulated data looking for photons or neutrinos coincident in time and direction with GRBs in a catalog, and examine all phases of the bursts in their field of view. MILAGRITO, the predecessor of MILAGRO reported detection of TeV gamma-rays in association with GRB 970417a [16] with

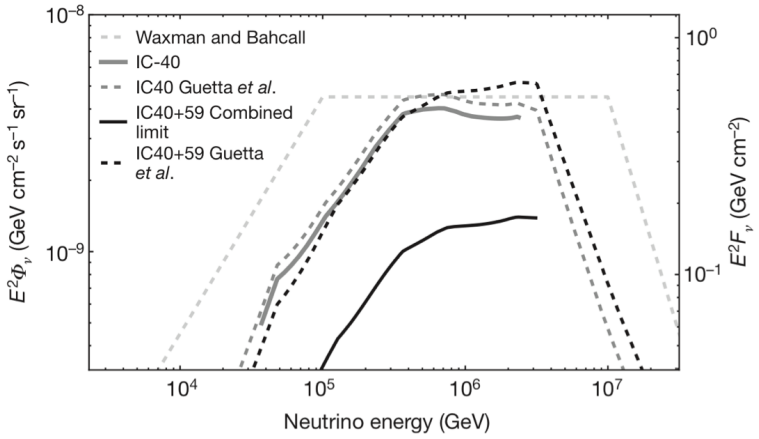

Fig. 2. IceCube limits on neutrinos associated with GRB [19].

a chance probability of 1.5×10^{-3}. Neither MILAGRO [17] nor IceCube [18] observed events in association with the bright "Naked Eye" GRB 080312B.

More constraining is the absence of any neutrino associated with 215 identified Northern hemisphere gamma-ray bursts between April 2008 and May 2010 [19]. The primary search was for ν_μ-induced upward muons from GRBs in the Northern hemisphere with IceCube-40 and IceCube-59. Figure 2 summarizes the result. The dashed lines show predictions of models normalized in different ways. The original Waxman-Bahcall calculation [20] relates the neutrino-producing protons to the observed spectrum of ultra-high energy cosmic rays under the assumption that GRB are the source of UHECR. Guetta et al. [21] made a detailed model which predicted a specific spectral shape for the neutrinos based on the observed break points in the spectrum of photons from the GRB, which are the target for photoproduction of neutrinos by accelerated protons. The neutrino spectrum is normalized in this model by assuming a certain relation between the energy density in electrons (which produce the observed photons primarily by synchrotron radiation) and the energy density in protons which are assumed to be accelerated along with the electrons. Using the latter model, individual predicted spectra were folded with the acceptance of IceCube and the results added to obtain the prediction shown. With this shape and normalization, 8 neutrino events were predicted and none were observed. The specific model has theoretical assumptions that have been challenged [22], and it has been argued that the predictions could be reduced by up to an order of magnitude. Nevertheless, the experimental limit is quite strong independent of any model.

The right ordinate shows the experimental limit on the fluence accumulated during 215 windows (averaging 28 seconds) around each burst. Assuming a total of 667 GRB per year, the fluence is converted to a limit on the all-sky flux of GRB neutrinos shown on the left ordinate. This limit is already more than an order of magnitude lower than the energy density in UHECR from Eq. 6, albeit at a lower energy per particle. The possible significance of this fact will be discussed in the conclusion.

4 Neutrinos from unresolved sources

Neutrinos are not absorbed therefore sources out to the Hubble radius will make roughly equal contributions from each spherical shell [24], so it is quite possible that many astrophysical neutrinos will be observed before a specific source is established. The spectra of astrophysical neutrinos should reflect the parent particle spectrum, perhaps $E^{-2.4}$ to E^{-2}. For these reasons it is worthwhile to look for a hard spectrum of neutrinos from unresolved astrophysical sources above the background of atmospheric neutrinos from decay of pions and kaons, which has a spectrum steepening from E^{-3} to E^{-4} as energy increases from the TeV to the PeV range.

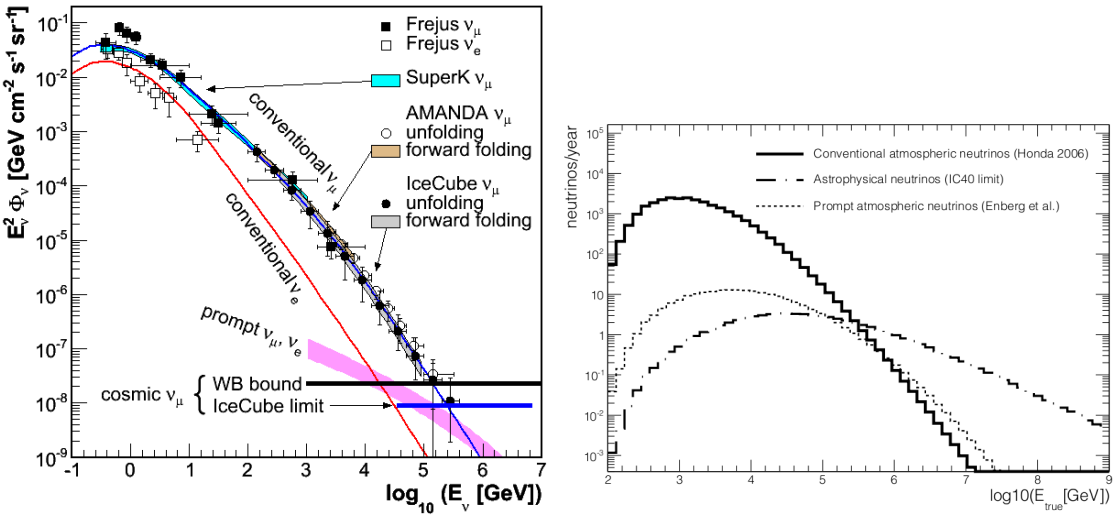

Fig. 3. Left: Atmospheric neutrinos compared to limits on astrophysical neutrinos. (K. Woschnagg for the IceCube Collaboration). Right: distribution of parent ν_μ energies for three components after applying the response of IceCube [23].

The highest event rate in all existing neutrino telescopes is the charged current ν_μ channel because the target volume is increased by interactions outside the detector, with high energy muons propagating several kilometers before crossing the detector. Current upper limits of this type from IceCube are now at the level of $E\mathrm{d}N_\nu/\mathrm{dln}\ E_\nu \approx 10^{-8}$ GeV cm^{-2}s^{-1}sr^{-1} [25]. The situation is shown schematically in Fig. 3. The Waxman-Bahcall bound [26] (shown by the heavy solid line in the figure) is an upper limit on the flux of astrophysical neutrinos that holds for sources of UHECR in which a fraction of the accelerated cosmic-rays photo-produce in the sources. The fraction of energy lost to interactions in which neutrinos are produced cannot be larger than, say $\frac{1}{2}$ or the sources would not be efficient cosmic-ray sources. The bound holds for AGN jets and GRBs. The solid blue line shows the current IceCube upper limit on an isotropic flux of ν_μ.

Figure 3 also illustrates several other important facts. The current upper limit crosses the atmospheric background around $E_\nu \approx 300$ TeV. This is high enough so that prompt neutrinos from decay of charm need to be considered as possible background along with the "conventional" neutrinos from decay of pions and kaons. It is also high enough so that the knee of the primary spectrum needs to be accounted for in calculating the atmospheric background.

The right panel of Fig. 3 shows the distributions of true neutrino energies for ν_μ folded with the response of the 59-string version of IceCube to neutrino-induced muons from below. The astrophysical component here is normalized at the level of the IC-40 limit [25]. Only the light produced by the muon traversing the detector is measured, which is directly related to the energy deposited by the muon. The analysis therefore proceeds by treating the normalizations and spectral slopes of the three components as parameters and fitting the observed energy deposition in the detector. Constraints reflecting the prior knowledge of the atmospheric neutrinos are placed on the range in which those parameters are allowed to vary. The difference in angular distributions between conventional and prompt atmospheric neutrinos is accounted for.

As a consequence of oscillations, it is expected that astrophysical neutrinos should contain all three neutrino flavors in comparable numbers. It is therefore essential to look in the ν_e and ν_τ channels even though the effective target volume is somewhat smaller than for ν_μ. As shown in the left panel of Fig. 3, atmospheric ν_e have a significantly steeper spectrum than ν_μ, so the atmospheric background in this channel is lower. A charged current interaction of a high energy electron neutrino produces a cascade that is contained within a few meters in water or ice, which means the event is almost spherically symmetric so that the energy of the neutrino itself can be directly inferred from the amount of light.

The ν_τ channel is essentially absent in atmospheric neutrinos at the high energies of interest here, so observation of a ν_τ would be a strong signal of astrophysical origin. As pointed out in Ref. [27], charged current interactions of τ-neutrinos lead to elongated (or at extremely high energy) separated depositions of energy. For example, at a PeV a τ has a mean pathlength of 50 meters before it decays, which would produce a significantly elongated event relative to the 125 m spacing between strings of IceCube. A description of how IceCube can identify ν_τ is given in Ref. [28]. Electron neutrinos in the hundred GeV range have been identified in the inner DeepCore subarray of IceCube [29]. Both cascade channels make important contributions to the limits set on neutrinos with energy in the PeV range and above [30]. Recently two ~PeV cascade events have been found in IceCube [31] and are being analyzed in detail.

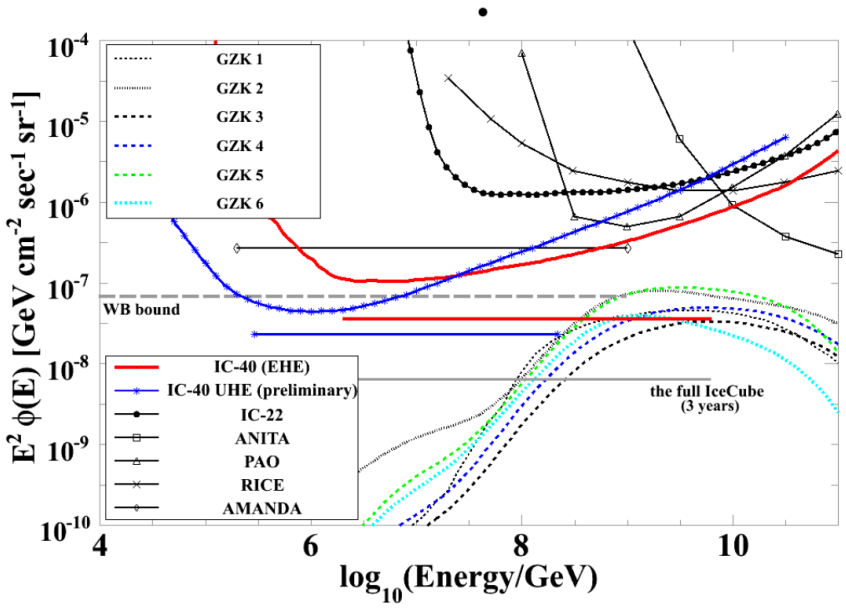

Fig. 4. Collection of limits on cosmogenic and ultra-high energy neutrinos. The plot is from Ref. [30] where full references are given. The extra curve included here, labeled *IC-40 UHE (preliminary)* is from Ref. [53].

5 Cosmogenic neutrinos

Whether or not accelerators of UHECR are also prolific neutrino sources, there will be neutrinos at some level produced outside their sources by

$$p + \gamma \to \Delta^+ \to n + \pi^+ \to \nu \\ \to p + \pi^0 \to \gamma\gamma \tag{4}$$

as the cosmic-rays propagate through the microwave background (CMB) and the extragalactic background light (EBL). In the CMB the cosmogenic neutrinos [32] are produced in the same processes that produce the suppression of the cosmic-ray flux above 5×10^{19} eV [33,34].

The level of cosmogenic neutrinos is in principle a sensitive probe of the origin of ultra-high energy cosmic rays. It depends on the spectrum injected by the sources, cosmological evolution of

the sources and the composition of the primary cosmic rays. If the primaries are almost all protons and if the spectrum in the source extends well above 10^{20} eV, then there will be significant production of cosmogenic neutrinos, but the intensity depends on the injected spectrum and on cosmological evolution of the sources [35,36]. One example of a proton only model is that of Ref. [37]. The ankle of the spectrum between 10^{18} and 10^{19} eV in this model is explained as a consequence of pair production by protons interacting with CMB photons. The model requires a fairly steep spectrum at the source, and the transition from galactic to extra-galactic cosmic rays is at quite low energy, around 3×10^{17} eV. The nearly pure proton composition of UHECR is consistent with the results reported by Hi-Res [38] and Telescope Array [39].

At the other extreme, it is possible to make a realistic model with combination of protons and iron assuming an exponential cutoff in rigidity of $R_{\rm max} \sim 5\times10^{18}$ V. The cutoff in energy for iron at the same rigidity is 26 times higher than for protons, i.e. $\sim 1.3\times10^{20}$ eV. This is the "disappointing" model of UHECR [40] motivated by the composition result reported by Auger [41] in which the composition changes from mostly protons at 10^{18} eV to mostly iron above 10^{19} eV. In this model, the sharp ankle is explained by the cutoff in protons and the transition to iron. In this case most nucleons would be below the threshold for photopion production on the CMB. There would then be only a low level of neutrinos from photoproduction on the higher frequency but lower density EBL.

The disappointing model is not the only solution in case the highest energy particles are largely heavy nuclei. The spectrum at the source may still extend well above 10^{20} eV for all species, and there would then be a steepening of the spectrum around 5×10^{19} eV, from photo-pion production for the protons and additionally from photodisintegration for the nuclei. Generally mixed composition models are associated with the Auger composition result and a galactic to extragalactic transition around the ankle just below 10^{19} eV, while the proton models are associated with the Hi-Res and TA composition result and a transition at lower energy [42].

The comprehensive paper of Ref. [36] explores the full range of possibilities for composition, transition energy and source evolution, subject to the constraint that each model fits the observed cosmic ray spectrum above 10^{19} eV. For example, it is also possible to have a model dominated by protons, but with a high-energy transition from galactic to extragalactic origin at the ankle. This requires a harder spectral index for the acceleration [35,36]. The range of predictions for all allowable ranges of assumptions varies over almost three orders of magnitude from one extreme to the other [36].

Current limits on cosmogenic neutrinos come from several types of measurements. The giant air shower experiments can identify neutrinos as late developing horizontal air showers (HAS). The best such limit is from Auger, where most of the contribution to the expected signal is from Earth skimming ν_τ in which the observed HAS is from decay of a τ-lepton emerging from the charged current interaction of a ν_τ [43]. Non-observation of late developing showers in the atmosphere also contribute somewhat to the limit [44].

Another approach is to look for signals in the radio band from neutrino interactions in the ice. This has been done with the RICE antennas buried in the ice at the South Pole [45], a method which is being expanded to much larger effective volume by with the Askaryan Radio Array now in the first phase of construction at the South Pole [46]. Another project with similar scope also in initial stages of deployment is ARIANNA on the Ross ice shelf to look for signals of neutrino interactions in the ice reflected from the ice-water interface [47]. The balloon born radio detector ANITA [48] has flown twice around Antarctica looking down at the ice for radio signals with polarization characteristic of neutrino interactions in the ice. One neutrino candidate with the expected vertical polarization was found in the second flight [49]. Analysis of the first flight, which accepted both polarizations, found 16 ultra-high energy cosmic ray cascade, but no neutrino candidates [50].

The upper limits from these experiments are shown along with the results from IceCube in Fig. 4 and with a selection of predictions for the spectrum of cosmogenic neutrinos. All the calculations shown are in the optimistic range of the calculations of Ref. [36]. The curve labeled GZK6 is a calculation [51] that estimates the maximum flux of cosmogenic neutrinos allowed by the diffuse γ background observed by the Fermi Satellite [52]. The π^0 channel in Eq. 4 produces high energy photons that cascade down to the GeV-TeV range and contribute to the diffuse gamma-ray background.

Limits shown in Fig. 4 are for the sum of three flavors assuming equal fluxes, as expected as a consequence of oscillations. Differential limits are obtained by assuming an E^{-2} spectrum over a

logarithmic bin of energy and calculating the limit for the each bin. The shapes of the curves then indicate the energy response of each detector. The limits for a full E^{-2} neutrino spectrum are shown as straight lines in the plot. The most precise result is to calculate the expected signal for each flux model and state the corresponding limit or expectation. For example, for the flux of Ref. [51] the expected number of events is 0.43 for IC-40 detector, which was half the size of the completed IceCube.

6 Conclusion

The IceCube upper limit on neutrinos from GRB obtained while the detector was under construction approaches the level of

$$E\frac{\mathrm{d}N_\nu}{\mathrm{d}\ln E_\nu} \approx 10^{-9}\,\mathrm{GeV\,cm^{-2}sr^{-1}s^{-1}}, \tag{5}$$

more than an order of magnitude below the energy density in cosmic rays in Eq. 6. The full IceCube with 86 strings has been in operation for more than a year, since May 2011. As analysis of data from the full detector proceeds, the sensitivity for neutrinos from the whole sky will reach this level. One can ask, if neutrinos are closely connected with the sources of ultra-high energy cosmic rays, what intensity should one expect?

A possible answer to this question can be given for compact accelerators like AGN jet or GRBs in which the accelerated protons are trapped by the turbulent magnetic fields that make the acceleration work. In such environments the protons would lose energy by photoproduction on the intense radiation fields inside the sources. Only neutral particles (neutrons, photons and neutrinos) would escape. The conditions in terms of optical depths for the various processes involved are given in Ref. [54]. The idea is also discussed specifically in connection with GRBs in [55]. Assuming the photoproduction is dominated by the Δ^+ resonance, the π^+ and the neutron will share the energy of the proton with a ratio of 0.28. After the $\pi^+ \to \mu^+ \to e^+$ decay sequence is complete, each of the three neutrinos will have on average 7% of the energy in the neutron. Attributing the entire observed cosmic ray flux (Eq. 6) to the escaping neutrons would then give an estimate of the energy flux per neutrino flavor

$$E\frac{\mathrm{d}N}{\mathrm{d}\ln E} \approx 1.4\times 10^{-9}\,\mathrm{GeV\,cm^{-2}sr^{-1}s^{-1}} \tag{6}$$

assuming $\nu_\mu : \nu_e : \nu_\tau = 1:2:0 \to 1:1:1$.

A feature of this type of model is that the photoprodution threshold in the acceleration region would give a minimum energy for escaping neutrons and hence for their contribution to the extra-galactic cosmic rays [56]. The corresponding break in the neutrino flux would occur at perhaps a factor 20 lower energy with a shape similar to Fig. 2.

Acknowledgments

I am grateful helpful discussions with Markus Ahlers and Teresa Montaruli in preparing the talk on which this paper is based. I also thank Juanan Aguilar, Alexander Kappes, Francis Halzen and Todor Stanev for helpful discussions. This research is supported in part by the U.S. National Science Foundation Grant NSF-ANT-0856253.

References

1. R.U. Abbasi et al., Phys. Rev. Letters **100** (2008) 101101.
2. T. Abu-Zayyad et al., arXiv:1205.5067.
3. M. Takeda et al., Astropart. Phys. **19** (2003) 447.
4. J. Abraham et al., Phys. Lett. B **685** (2010) 239.
5. A.M. Hillas, Ann. Revs. Astron. & Astrophysics, **22** (1984) 425.

6. IceCube Collaboration (R. Abbasi et al.) Ap.J. **732** (2011) 18.
7. V.A. Acciari et al., Ap.J. **729** (2011) 2.
8. W. Benbow (for the VERITAS Collaboration), Proc. 32nd Int. Cosmic Ray Conf. (Beijing, 2011) arXiv:1110.0038.
9. http://tevcat.uchicago.edu/
10. J.A. Aguilar, presentation at SciNiGHE 2012 (Lecce, Italy, June 2012).
11. H. Krawczynski et al., Ap.J. **601** (2004) 151. See also J. Holder et al., Ap.J. **583** (2003) L9.
12. M. Böttcher Astrophys. Space Sci. **309** (2007) 95.
13. VERITAS Collaboration (V.A. Acciari et al.) Ap.J. **743** (2011) 62.
14. A.A. Abdo et al. (Milagro Collaboration), Ap.J. **666** (2007) 361.
15. HAWC Collaboration (A.U. Abeysukara et al.) Astropart. Phys. **35** (2012) 641.
16. R. Atkins et al., Ap.J. **583** (2003) 824. See also R. Atkins et al., Nucl. Instrum. Methods Phys. Res. A, **449** (2000) 478
17. T. Aune, Saz Parkinson for the MILAGRO Collaboration, Proc. 31st Int. Cosmic Ray Conf. (Lodz) 2009.
18. IceCube Collaboration, R. Abbasi et al., Ap.J. **701** (2009) 1721 (Erratum, **708** (2010) 911).
19. IceCube Collaboration (R. Abbasi et al.) Nature **484** (2012) 351.
20. E. Waxman & J. Bahcall, Phys. Rev. Letters **78** (1997) 2292.
21. D. Guetta et al., Astropart. Phys. **20** (2004) 429.
22. S. Hümmer, P. Baerwald & W. Winter, arXiv:1112.1076v3.
23. IceCube Collaboration (A. Schukraft, S. Grullon, M. Wallraff), Proc. 32nd ICRC (Beijing, 2011) arXiv:112736.
24. P. Lipari, Phys. Rev. D **78** (2008) 083011.
25. IceCube Collaboration (R. Abbasi et al.) Phys. Rev. D **84** (2011) 082001/
26. E. Waxman & J. Bahcall, Phys. Rev. D **59** (1998) 012002.
27. J.G. Learned & S. Pakvasa, Astropart. Phys. **3** (1995) 267.
28. IceCube Collaboration (R. Abbasi et al.) arXiv:1202.3039.
29. C. Ha for the IceCube Collaboration, arXiv:1201.0801.
30. R. Abbasi et al. (IceCube Collaboration), Phys. Rev. D **83**, 092003 (2011).
31. Aya Ishihara, presentation at Neutrino 2012, Kyoto, Japan.
32. V.S. Berezinsky & G.T. Zatsepin, Phys. Lett. **28** B (1969) 423.
33. K. Greisen, Phys. Rev. Letters **16** (1966) 748.
34. G.T. Zatsepin & V.A. Kuz'min, JETP Lett. **4** (1966) 78.
35. D. Seckel & T. Stanev, Phys. Rev. Letters **95** (2005) 141101.
36. K. Kotera, D. Allard & A.V. Olinto, JCAP (2010) 10-013.
37. V. Berezinsky, A. Gazizov & S. Grigorieva, Phys. Rev. D **74** (2006) 043005.
38. R.U. Abbasi et al., Phys. Rev. Letters **104** (2010) 161101.
39. Y. Tsunesada, Proceedings of the 32nd ICRC, Beijing, 2011, **12** 58.
40. R. Aloisio, V. Berezinsky & A. Gazizov, Astropart. Phys. **34** (2011) 620.
41. J. Abraham et al., (Pierre Auger Collaboration) Phys. Rev. Letters **104** (2010) 091101.
42. D. Allard, arXiv:0906.3156.
43. Y. Guardincerri for the Pierre Auger Collaboration, Proc. ICRC 2011 (Beijing) (arXiv:1107.4805).
44. Pierre Auger Collaboration (P. Abreu et al.), Phys. Rev. D **84** (2011) 122005 and Erratum D **85** (2012) 29902(E).
45. I. Kravchenko et al., arXiv:1106.1164.
46. P. Allison et al., arXiv:1105.2854.
47. S. Klein for the ARIANNA Collaboration, arXiv:1207.3846.
48. P. Gorham et al., Phys. Rev. D **82**, 022004 (2010).
49. P. Gorham et al., arXiv:1011.5004.
50. S. Hoover et al., arXiv:1005.0035v2.
51. M. Ahlers et al., Astropart. Phys. **34**, 106 (2010).
52. A.A. Abdo et al., Phys. Rev. Lett. **104**, 101101 (2010).
53. *Searching for an Ultra High-Energy Diffuse Flux of Extraterrestrial Neutrinos with IceCube 40*, H. Johansson, Ph.D. Thesis, University of Stockholm (2011).

54. M. Ahlers, L.A. Anchordoqui & S. Sarkar, Phys. Rev. D **79** (2009)083009.
55. M. Ahlers, M.C. Gonzalez-Garcia & F. Halzen, Astropart. Phys. **35** (2011) 87.
56. M. Ahlers & J. Salvado, arXiv:1105.5113 and M. Ahlers, private communication.